http://dx.doi.org/10.5012/bkcs.2013.34.1.128

Synthesis, Optical and Electrical Studies of Nonlinear Optical Crystal: L-Arginine Semi-oxalate

P. Vasudevan,[†,‡] S. Sankar,[†,*] and D. Jayaraman[§]

Department of Physics, MIT Campus, Anna University, Chennai -600 044, India. [*]E-mail:ssankarmit@gmail.com
[‡]Department of Physics, SKR Engineering College, Chennai -600 123, India
[§]Department of Physics, Presidency college, Chennai- 600 005, India
Received September 6, 2012, Accepted October 17, 2012

L-Arginine semi-oxalate (LASO) single crystal has been grown by solution growth technique at room temperature. The crystal structure and lattice parameters were determined for the grown crystal by single crystal X-ray diffraction studies. Photoluminescence studies confirm the violet fluorescence emission peak at 395 nm. Optical constants like band gap, refractive index, reflectance, extinction coefficient and electric susceptibility were determined from UV-VIS-NIR spectrum. The dielectric constant, dielectric loss and ac conductivity of the compound were calculated at different temperatures and frequencies to analyze the electrical properties. The solid state parameters such as plasma energy, Penn gap, Fermi energy and polarizability were calculated to analyze second harmonic generation (SHG). Nonlinear optical property was discussed to confirm the SHG efficiency of the grown crystal.

Key Words : Solution growth, Optical constants, Non-linear optical property

Introduction

In the recent years, the search for nonlinear optical (NLO) materials find considerable interest among the researchers due to their important impact on laser technology, fiber optic communication, optical modulation and optical data storage technology.[1] Among NLO materials, organic and semi-organic NLO materials are generally believed to be more versatile due to their more favorable nonlinear response on comparison with their inorganic counterpart. The nonlinear optical property of amino acid family of L-arginine crystals has motivated the researchers to grow and characterize the new compound of this family of crystals.[2-7] According to earlier reports,[8,9] L-arginine additions have second harmonic efficiency larger than potassium dihydrogen phosphate (KDP). Recently, some crystalline salts of L-arginine with organic acids were grown and characterized.[10-14] Many oxalate complex crystals are reported to be active in second harmonic generation[15] and it may also be useful to study the oxalates with other carboxylic acids and their properties. Oxalic acid with considerable π-conjugation has attracted our attention. With an interest to discover novel crystals of better NLO properties, we have grown L-arginine semi-oxalate crystals by slow evaporation technique at room temperature. The structure of LASO was first reported by Chandra *et al.*[16] It belongs to triclinic crystal system with space group P_1 and cell parameters a = 5.06 (14) Å, b = 9.75(13) Å, c = 13.14(3) Å; α = 111.11(2)°, β = 92.75(3)°, γ = 91.97(3)° and cell volume 604.4(2) Å^3. The literature survey reveals that the other studies except structure are not available for the grown material LASO. Hence, we have taken initiatives in the present investigation to explore the optical and electrical properties of the title compound for analyzing NLO property.

Experimental

L-Arginine semi-oxalate single crystal was formed in aqueous solution containing L-arginine (Loba chemie-99%) and oxalic acid dihydrate (Loba chemie-99%) in molar ratio 1:1 at room temperature. Calculated amount of reactants were thoroughly dissolved in double distilled water and stirred well by using magnetic stirrer to ensure homogeneous solution. The solution was then filtered using filter paper and transferred to a Petri dish. The prepared solution was allowed to evaporate at room temperature. The growth was initiated due to slow evaporation of the solvent. The quality of the crystal was improved by recrystallization process. After a period of 45 days, transparent good quality of the crystal was harvested. The grown crystal with dimension 10 × 9 × 2 mm^3 is shown in Figure 1. The reaction procedure for the formation of the crystal is given by

$$C_6H_{14}N_4O_2 + C_2H_2O_4{\cdot}2H_2O \rightarrow C_6H_{15}N_4O_2^{+}{\cdot}C_2HO_4^{-} \quad (1)$$

Figure 1. Photograph of as-grown LASO crystal.

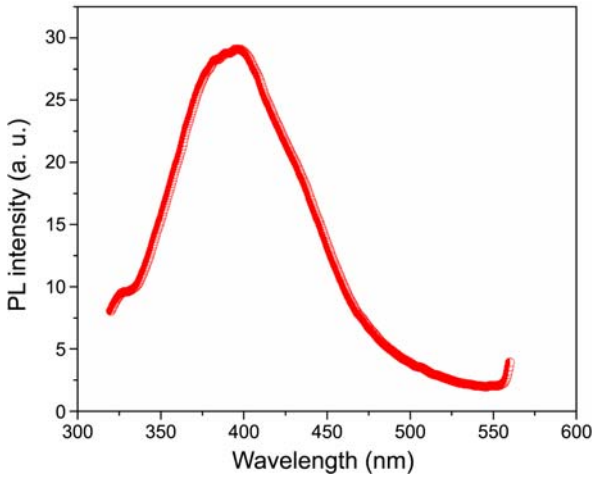

Figure 2. Emission spectrum of LASO crystal.

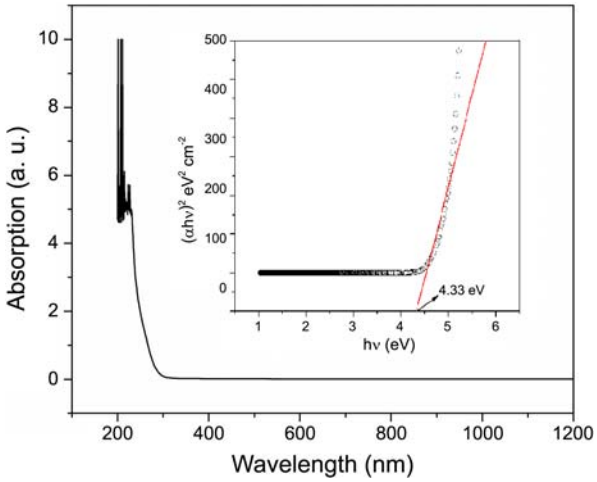

Figure 3. UV-VIS-NIR absorption spectrum of LASO crystal.

Single crystal XRD studies were carried out using Bruker Kappa APE XII single X-ray diffractometer to determine the lattice parameters and the space group. Fluorescence spectra were recorded with the help of Perkin Elmer LS45UV fluorescence spectrophotometer. Optical absorption measurements were made using Perkin Elmer Lamda 35 UV-VIS-NIR spectrophotometer with a resolution of 2 nm in the region from 200 nm to 1200 nm to measure the absorption range of the crystal. Dielectric studies were carried out to an accuracy of ± 2% using a HIOKI LCR Hitester in the frequency range from 100 Hz to 5 MHz. Nonlinear properties of LASO crystals was confirmed by Kurtz and Perry powder technique using Q-switched high energy Nd:YAG laser (QUANTA RAY model LAB-170-10).

Results and Discussion

Single Crystal X-ray Diffraction. The single crystal XRD data of LASO crystal confirm that it crystallizes in triclinic system with non-centrosymmetric space group P_1. The calculated lattice parameters are a = 5.05 Å, b = 9.73 Å, c = 13.12 Å, α = 111.03°, β = 92.79°, γ = 91.91° and the unit cell volume V = 600 Å^3. The XRD data of the crystal is found to be in good agreement with the reported values.[16]

Photoluminescence Studies. Photoluminescence study is a non-destructive tool to carry out the luminescence behaviour of the grown optical material. The recorded emission spectrum of LASO crystal in the range from 300 to 550 nm is shown in Figure 2, after exciting the sample at 325 nm. From the emission spectrum, a broad peak was observed at 395 nm. The result indicates that the LASO crystal has violet fluorescence emission. The maximum intensity peak at 395 nm is attributed to n-π* transition of carbonyl group. The presence of carbonyl group is thus confirmed.

Optical Constants. UV-VIS-NIR absorption spectrum was recorded in the wavelength range between 200 nm and 1200 nm (Figure 3). From the absorption spectrum, the lower cut-off wavelength is found to be 250 nm and the lower percentage absorption indicates that the crystal readily allows the transmission of the laser beam in the range between 250 nm and 1200 nm. It shows that the grown crystal has a good transparency in UV, visible and near IR region indicating that it can be used for NLO applications. Hence it is concluded that the grown crystal can be used for optoelectronic applications. The energy gap (E_g) was calculated as 4.33 eV from the plot of hν (h = Planck's constant, and, ν = frequency of light) *versus* $(\alpha_a h\nu)^2$ (α_a = absorption coefficient of material) shown in the inset of Figure 3. The relation between refractive index (n) and energy gap (E_g) is given by Reddy *et al.*[17] as

$$E_g e^n = 36.3 \quad (2)$$

After finding the refractive index, the reflectance (R) of the crystal was calculated using the expression

$$R = \left(\frac{n-1}{n+1}\right)^2 \quad (3)$$

The refractive index and reflectance of the crystal were calculated as 2.12 and 0.128 respectively in the transmission range. The refractive index of the grown crystal LASO has also been experimentally determined as 1.85 for the face (010) using the well known Brewster angle method as done recently by Vasudevan *et al.*[18] The calculated theoretical value, 2.12 (using Eq. (2)), is thus found to be in close agreement with the experimentally determined value. No significant variation was observed in the refractive index for the other two faces (100) and (001). The high value of refractive index and low value of reflectance reveal that the grown crystal is more transparent to transmit the light from 250 to 1200 nm. The extinction coefficient (K) was estimated using the following relation,

$$K = \frac{\alpha_a \lambda}{4\pi} \quad (4)$$

Figure 4 shows the plot of wavelength (nm) *versus* extinction coefficient (K). It is observed that as the wavelength increases, extinction coefficient decreases up to 250 nm and remains constant thereafter. This means the absorbance is

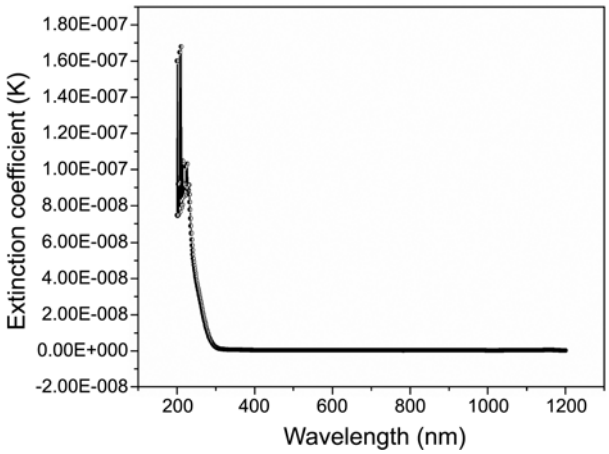

Figure 4. Variation of extinction coefficient with wavelength.

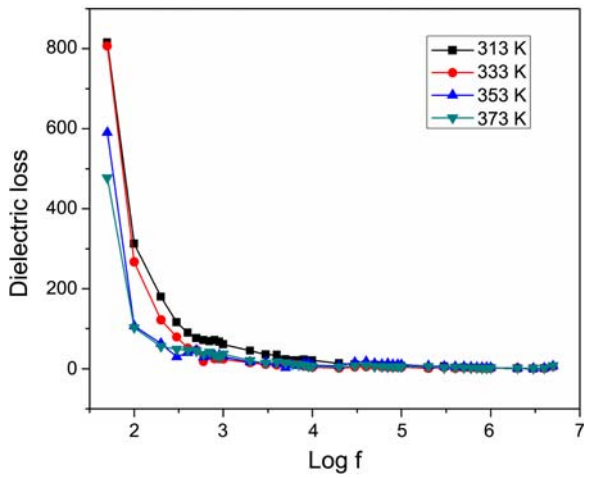

Figure 6. Variation of dielectric loss with frequency at various temperatures.

low in the visible and near IR region. This prediction is also confirmed from UV-VIS-NIR spectrum. Hence the grown crystal LASO can easily transmit the wavelength range from 250 to 1200 nm.

The electrical susceptibility (χ_c) was calculated using the following relation,

$$\chi_c = \varepsilon_r - 1 \quad (5)$$

or $$\chi_c = n^2 - 1 \quad (\therefore \varepsilon_r = n^2) \quad (6)$$

Hence, $\chi_c = 3.49$

Since electrical susceptibility is greater than 1, the material can be easily polarized when the incident light is more intense.

Dielectric Studies. The capacitance and dissipation factor of the sample were measured for various frequencies, in the range 100 Hz to 5 MHz. Dielectric constant (ε_r), dielectric loss (tanδ) were calculated using the relations $\varepsilon_r = Cd/\varepsilon_o A$ and $\tan\delta = \varepsilon_r D$ and shown in Figures 5 and 6. It is observed that the ε_r and tanδ values are found to decrease with the increase in frequency at all temperatures. The high value of ε_r at low frequency may be due to presence of all polarizations and its low value at higher frequencies may be due to the significant loss of all polarizations gradually.[19] In accordance with Miller rule, the lower value of dielectric constant is a suitable parameter for the enhancement of SHG efficiency. The variation of ε_r with temperature is generally attributed to the crystal expansion, the electronic and ionic polarizations and the presence of impurities and crystal defects.[20] The observed lower values of dielectric loss at higher frequencies for this sample suggest that the grown crystal contains less number of defects with high optical quality.[21]

The ac conductivity (σ_{ac}) has been calculated for the LASO crystal from the following formula $\sigma_{ac} = \varepsilon_o \varepsilon_r \omega \tan\delta$ where ε_o is the vacuum dielectric constant (8.85×10^{-12} farad/m), ε_r is the relative dielectric constant and ω is the angular frequency ($\omega = 2\pi\nu$) of the applied field. Figure 7 shows the variation of ac conductivity with various frequencies and temperatures. It is seen that the value of ac conductivity increases with increase in frequency. The elec-

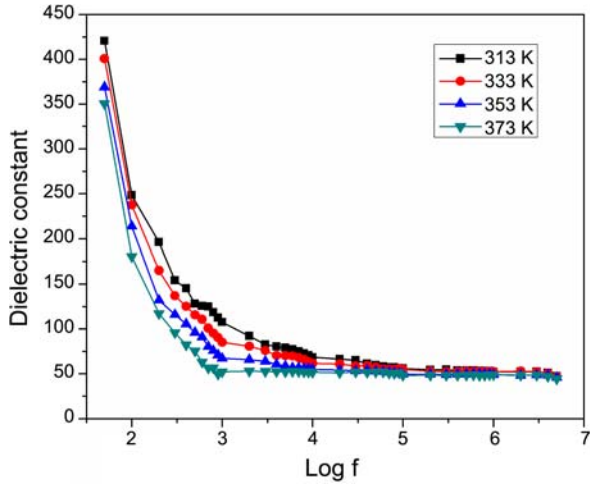

Figure 5. Variation of dielectric constant with frequency at various temperatures.

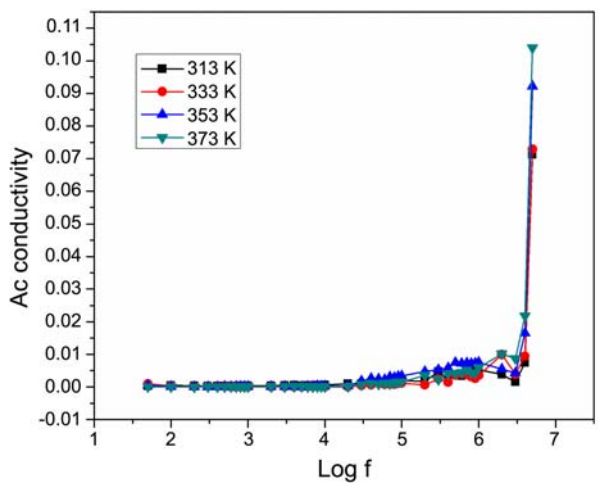

Figure 7. Variation of ac conductivity with frequency at various temperatures.

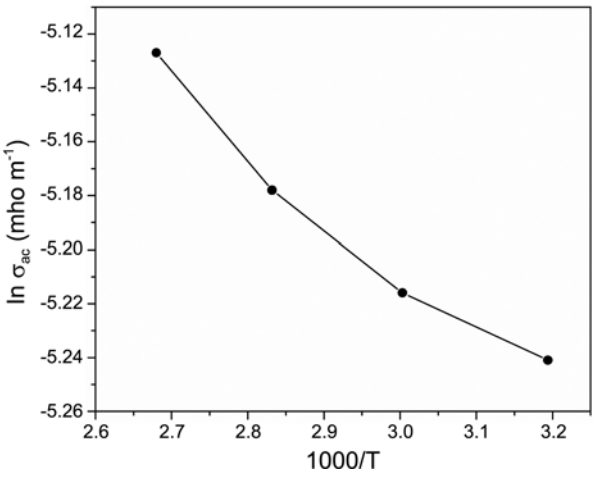

Figure 8. Activation energy of LASO crystal.

tronic exchange of the number of ions in the crystal gives local displacement of electrons in the direction of the applied field, which in turn gives rise to polarization. The slope of the plot of ac conductivity *versus* temperature (Figure 8) gives the activation energy required for the conduction process of the charge carriers. The value is found to be 0.218 eV and the lower value of activation energy establishes that the crystal contains less number of defects. The material is therefore useful for various microelectronic and nonlinear optical applications.

Solid State Parameters. Solid state parameters are necessary to analyse second harmonic generation efficiency of the title compound. From the single XRD data, the molecular weight (M) and density (ρ) are given as 264.25 and 1.452 g cm^{-3} respectively. The value of dielectric constant at 1 MHz is found to be $\varepsilon_\infty = 53.13$ from dielectric studies. The valence electron plasma energy ($\hbar\omega_P$) is given as

$$\hbar\omega_P = 28.8\left(\frac{Z\rho}{M}\right)^{1/2} \tag{7}$$

where Z is the total number of valence electrons (104), $\hbar = h/2\pi$ and ω_P is plasma angular frequency. The Penn gap (E_P) and Fermi energy (E_F) are given as follows[22]:

$$E_P = \frac{\hbar\omega_P}{(\varepsilon_\infty - 1)^{1/2}} \tag{8}$$

and

$$E_F = 2.948(\hbar\omega_P)^{4/3} \tag{9}$$

The polarizability (α_P) of the grown crystal can be obtained using the following relation[22]

$$\alpha_P = \left[\frac{(\hbar\omega_P)^2 S_0}{(\hbar\omega_P)^2 S_0 + 3E_P^2}\right] \times \frac{M}{\rho} \times 0.396 \times 10^{-24} \tag{10}$$

where

$$S_o = 1 - \left[\frac{E_P}{4E_F}\right] + \frac{1}{3}\left[\frac{E_P}{4E_F}\right]^2$$

The value of polarizability can also be estimated using

Table 1. Solid state parameters of LASO crystal

Parameters	Values for LASO crystal	Values for KDP crystal
Plasma energy (eV)	21.77	17.33
Penn gap (eV)	3.01	2.39
Fermi energy (eV)	17.92	12.02
Polarizability by Penn gap (cm^3)	6.79×10^{-23}	2.14×10^{-23}
Polarizability by Clausius-Mosotti equation (cm^3)	6.82×10^{-23}	2.18×10^{-23}

Clausius-Mosotti equation,

$$\alpha_P = \frac{3M}{4\pi N}\frac{\varepsilon_\infty - 1}{\varepsilon_\infty + 2} \tag{11}$$

where N_a is Avogadro number. The required solid state parameters for interpreting SHG efficiency have been computed using the Eqs. (7), (8), (9), (10) and (11). These values are compared with those of standard material KDP and listed in Table 1. From the table, it is observed that solid state parameters are found to be higher than those of KDP. In particular, the polarizability of LASO is found to be 1.5 times higher than that of KDP. As the SHG efficiency depends upon the polarizability, the SHG efficiency is also found to be 1.5 times more than that of KDP.

Second Harmonic Generation. The experiment of second harmonic generation efficiency was performed using Kurtz and Perry powder technique with Nd:YAG laser source of wavelength 1064 nm.[23] The grown crystal of LASO was crushed to fine powder and placed in a microcapillary of uniform bore. A high intensity laser radiation was passed through the sample. The SHG efficiency of LASO was compared with that of KDP from the output power. The ratio of SHG efficiency of LASO to that of KDP is found to be 1.5. The experimental result is thus found to be in good agreement with the theoretically predicted result discussed in the previous section.

Conclusion

L-Arginine semi-oxalate single crystal was successfully grown by slow evaporation technique. From XRD data, it is observed that the grown crystal belongs to triclinic structure and non-centrosymmetric space group P_1. Photoluminescence spectrum shows that the material has violet fluorescence emission at 395 nm. The band gap, refractive index, reflectance, extinction coefficient and electrical susceptibility were calculated to analyze the optical property. Dielectric studies establish the dielectric behaviour of the grown material. The solid state parameters such as plasma energy, Penn gap, Fermi energy and polarizability were calculated. The higher value of polarizability indicates that the second harmonic generation efficiency is more than that of standard material KDP. The theoretical prediction of SHG efficiency was confirmed by Kurtz and Perry powder technique.

Acknowledgments. One of the authors P. Vasudevan wishes

to thank the Chairman Sri M. Srinivasan and the Managing Trustee Sri K. Ramadoss of the Srinivasa Educational Trust, for their support.

References

1. Misoguti, L.; Varela, A. T.; Nunes, F. D.; Bagnato, V. S.; Melo, F. F. A.; Mendes Filho, J.; Zilio, S. C. *Opt. Mater.* **1996**, *6*, 147.
2. Monaco, S. B.; Devis, L. E.; Velsko, S. P.; Wang, F. T.; Eimerl, D.; Zalkin, A. *J. Cryst. Growth* **1987**, *85*, 252.
3. Sangeetha, K.; Ramesh Babu, R.; Bhagavannarayana, G.; Ramamurthy, K. *Mater. Chem. Phys.* **2011**, *130*, 487.
4. Hameed, A. S. H.; Ravi, G.; Ramasamy, P. *J. Cryst. Growth* **2001**, *229*, 547.
5. Vasantha, K.; Dhanushkodi, S. *J. Cryst. Growth* **2004**, *269*, 333.
6. Terzyan, S. S.; Karapetyan, H. A.; Sukiasyan, R. B.; Petrosyan, A. M. *J. Cryst. Growth* **2004**, *687*, 111.
7. Renuka, N.; Vijayan, N.; Rathi, B.; Ramesh Babu, R.; Nagarajan, K.; Harinath, D.; Bhagavannarayana, G. *Optik* **2012**, *123*, 189.
8. Baraniraj, T.; Philominathan, P. *Spectrochim. Acta, Part A* **2010**, *75*, 74.
9. Petrosyan, A. M.; Sukiasyan, R. P.; Karapetyan, H. A.; Terzyan, S. S.; Feigelson, R. S. *J. Cryst. Growth* **2000**, *213*, 103.
10. Suresh, C. G.; Vijayan, M. *Int. J. Peptide Protein Res.* **1983**, *21*, 223.
11. Bhat, T. N.; Vijayan, M. *Acta Crystallogr. B* **1977**, *33*, 1754.
12. Suresh, C. G.; Ramaswamy, J.; Vijayan, M. *Acta Crystallogr.* **1986**, *B 42*, 473.
13. Soman, J.; Vijayan, M. *J. Biosci.* **1989**, *14*, 111.
14. Ravishankar, R.; Chandra, N. R.; Vijayan, M. *J. Biomed. Struct. Dyn.* **1998**, *15*, 1093.
15. Bhat, H. L. *Bull. Mater. Sci.* **1994**, *17*, 1233.
16. Chandra, N. R.; Prabu, M. M.; Venkataraman, J.; Suresh, S.; Vijayan, M. *Acta Crystallogr., Sect. B* **1998**, *54*, 257.
17. Reddy, R. R.; Anjaneyulu, S. *Phys. Stat. Solidi.* **1992**, *174*, 91.
18. Vasudevan, V.; Ramesh Babu, R.; Reicher Nelcy, A.; Bhagavannarayana, G. *Bull. Mater. Sci.* **2011**, *34*, 469.
19. Smyth, C. P. *Dielectric Behaviour and Structure*; McGraw-Hill: New York, 1965; p 132.
20. Priya, M.; Mahadevan,C. K. *Cryst. Res. Technol.* **2009**, *44*, 92.
21. Balarew, C.; Duhlew, R. *J. Solid State Chem.* **1984**, *55*, 1.
22. Ravindra, N. M.; Bharadwaj, R. P.; Sunil Kumar, K.; Srinivastava, V. K. *Infrared Phys.* **1981**, *21*, 369.
23. Kurtz, S. K.; Perry, T. T. *J. Appl. Phys.* **1968**, *39*, 3798.